Biosensors and Bioelectronics 131 (2019) 200–206

Contents lists available at ScienceDirect

Biosensors and Bioelectronics

journal homepage: www.elsevier.com/locate/bios

An electrochemical sensor based on electro-polymerization of caffeic acid and Zn/Ni-ZIF-8–800 on glassy carbon electrode for the sensitive detection of acetaminophen

Wanqing Zhang[a,*], Lukuan zong[b], Shanqin Liu[a], Shuai pei[a], Yongsheng Zhang[b], Xiaoman Ding[a], Bo Jiang[a], Yuping Zhang[a,*]

[a] School of Chemistry and Chemical Engineering, Henan Institute of Science and Technology, Xinxiang 453003, China
[b] School of Chemical Engineering and Energy, Zhengzhou University, Zhengzhou 450001, China

ARTICLE INFO

Keywords:
PCA@ Zn/Ni-ZIF-8–800/GCE sensor
Electro-polymerization method
Synergistic effect
Electrochemical detection
Acetaminophen

ABSTRACT

A new electrochemical sensor was fabricated for the sensitive and selective detection of acetaminophen (AP), based on a bare glassy carbon electrode (GCE) modified with poly caffeic acid (PCA) and Zn/Ni-ZIF-8–800 using an electro-polymerization method. The carbon material of Zn/Ni-ZIF-8–800 derived from bimetal-organic framework was synthesized by one-step pyrolysis method. Then, the as-prepared materials and the corresponding fabricated sensors were fully characterized by XRD, FTIR, BET, SEM, TEM and XPS analyses. In addition, the electron transfer abilities of the modified sensors were investigated by CV and EIS. Subsequently, the parameters of polymerization time, pH value and scan rate were systematically studied and optimized. Under the optimum conditions, the desirable linear relationships were obtained between the peak current and the AP concentration at the PCA@ Zn/Ni-ZIF-8–800/GCE sensor with a detection limit of 0.0291 μM. The outstanding electrochemical performance of the proposed sensor can be attributed to the good electrocatalytic activity of PCA, the large surface area and high conductivity of Zn/Ni-ZIF-8–800 as well as the synergistic effect of PCA and Zn/Ni-ZIF-8–800. Moreover, the fabricated sensor was also successfully applied for the determination of AP in pharmaceutical dosage forms and human urine sample, and satisfactory recoveries were obtained.

1. Introduction

Acetaminophen (AP, N-acetyl-p-aminophenol), is an analgesic and antipyretic drug which is usually used for the treatment of fevers and relief of pain. Its pharmacological effects are based on its inhibition of the synthesis of prostaglandins (Wang et al., 2007; Adhikari et al., 2015; Cernat et al., 2015). Generally, suitable administration of AP doses is safe and does not have any harmful side effects on the health of the body. However, ingestion of excessively high doses or long-term usage of AP can lead to the accumulation of toxic metabolites, reducing the liver's ability to detoxify and causing a number of health problems such as fatal hepatotoxicity and nephrotoxicity (Habibi et al., 2011; Lu et al., 2012). Therefore, the development of a facile, sensitive and accurate method to determine AP has gained increasing research interests. To date, different kinds of analytical techniques have been reported for the detection of AP, such as spectrophotometry (Glavanovic et al., 2016), high-performance liquid chromatography (HPLC) (Nebot et al., 2007), titrimetry (Girish Kumar, Letha, 1997), chemiluminescence (Ruengsitagoon et al., 2006), fluorimetry (Vilchez et al., 1995) and capillary electrophoresis (CE) (Perez-Ruiz et al., 2005), etc. However, some of these methods have the disadvantages of large time consumption, high cost tedious sample pretreatment and low sensitivity. In contrast, electrochemical methods have easy operation, quick response and high selectivity, and are being considered for the sensitive and selective detection of AP (Zhang et al., 2016; Alam et al., 2018).

Nevertheless, the electrochemical response of AP is not obvious at bare glassy carbon electrode (GCE). Therefore it is necessary to introduce some electrode modifiers to improve the sensitivity of GCE. To the best of our knowledge, the earliest reports of electrochemical detection of AP can be traced back to 1992, in which a sensor modified with glucose oxidase was fabricated (Moatti-Sirat et al., 1992). Since then, various materials have been widely used to modify GCE, including MWCNT (Alothman et al., 2010), GO (Zidan et al., 2014), metals (Boopathi et al., 2004), metal oxides (Mazloum-Ardakani et al., 2010), metal/carbonaceous hybrids (Wang et al., 2007), metal oxide/

* Corresponding authors.
E-mail addresses: zhangwqzzu@163.com (W. Zhang), beijing2008zyp@163.com (Y. Zhang).

https://doi.org/10.1016/j.bios.2019.01.069
Received 22 November 2018; Received in revised form 14 January 2019; Accepted 27 January 2019
Available online 19 February 2019
0956-5663/

carbonaceous hybrids (Sivakumar et al., 2016) and composites (Chen et al., 2016). For example, Cao et al. prepared an electrochemical sensor based on screen-printed electrode modified with $Ce_{0.75}Bi_{0.25}O_x$ for the determination of AP, which achieved a high sensitivity of 360 μA μM cm^{-2} (Cao et al., 2018). In another study, a NiO/CNTs/DPID/CPEs sensor was fabricated by Karimi-Maleh and used to monitor AP, which showed a wide linear detection range from 0.8 to 550 μM and a low detection limit of 0.3 μM (Karimi-Maleh et al., 2017). Wang et al. constructed an electrochemical sensor using Au/Pd/rGO nanohybrid modified GCE for the detection of AP (Wang et al., 2018). The proposed sensor exhibited a wide linear range, low detection limit and high sensitivity, and was successfully applied for the determination of AP in real samples with good satisfactory recoveries (Chandra et al., 2013; Adhikari et al., 2015). According to the reviewed literature, mumerous modifiers have been used to promote the electrochemical response of AP at the modified electrode sensors.

Recently, a large number of reports in the electrochemical fields have been published with redox polymers as sensor modifiers (Xu et al., 2012). Poly caffeic acid (PCA), one of the redox polymers possessing outstanding features of high sensitivity, excellent catalytic activity and good selectivity has been widely applied in the application of electrocatalysis and electrochemical sensors. Moreover, when PCA was used as a sensor modifier, it could catalyze the reduction of target molecules and participate in reversible electron transfer in electrochemical reaction process (Ates, 2013; Lee and Compton, 2013).

Metal-organic frameworks (MOFs), a class of highly ordered porous materials consisting of metal ions (or metal clusters) and organic ligands, have been attracted enormous attention in recent years (Khan et al., 2013; Zhang et al., 2018a, 2018b, 2018c). Due to their unique features of appropriate pore volume, ultra-high surface area, large pore size, rich topologies and high porosity, MOFs have been widely used in various applications such as gas adsorption/separation (Juan-Juan et al., 2010), supercapacitors (Liu et al., 2010), catalysis device (Wu et al., 2017), sensors (Zhang et al., 2018a, 2018b, 2018c) and batteries (Shi et al., 2017). Carbon materials derived from MOFs (C-MOFs) possess larger surface area, higher conductivity as well as better thermodynamic and mechanical stability than the original framework structure material. Consequently, they have been introduced in the fabrication of electrochemical sensors (Zhao et al., 2017; Kim et al., 2018). Zn/Ni-ZIF-8-800, a typical C-MOFs, was selected as the modifier in this study for the following reasons: (i) Zn and Ni can easily form an alloy after a simple carbonization process, providing Zn/Ni-ZIF-8-800 with good conductivity; (ii) the material is beneficial for accelerating the electron transfer between the AP and the electrochemical sensor; (iii) the Zn/Ni-ZIF-8-800 can provide a suitable place to prompt the redox reaction of AP under the electrocatalytic effect of PCA. The introduction of Zn/Ni-ZIF-8-800 can make the PCA@Zn/Ni-ZIF-8-800 hybrid possess high conductivity and large surface area. To the best of our knowledge, an electrochemical sensor based on bare GCE modified with PCA and Zn/Ni-ZIF-8-800 for the detection of AP has not been reported yet.

In this paper, an electrochemical sensor based on PCA and Zn/Ni-ZIF-8-800 modified bare GCE was fabricated by electro-polymerization method and employed for the determination of AP. The as-prepared materials and the corresponding sensors were thoroughly characterized by several techniques. Also, the experimental parameters of electrochemical measurements were explored in detail by various analytical methods. The excellent electrochemical performance of the proposed sensor for the detection of AP can be ascribed to the synergistic effect of PCA and Zn/Ni-ZIF-8-800. PCA can catalyze the redox of AP to significantly increase the sensitivity of PCA@Zn/Ni-ZIF-8-800 sensor due to its excellent electrocatalytic activity. Furthermore, the Zn/Ni-ZIF-8-800 with high surface area and suitable pore volume can provide a favorable reaction place, which could be helpful to catalyze AP in solution with PCA film at the electrochemical sensor.

2. Experimental section

Detailed information related to the reagents, instruments, electroanalytical measurements and preparation of real samples are presented in the Supporting information (Section S.1).

2.1. Synthesis of Zn/Ni-ZIF-8-800

The Zn/Ni-ZIF-8-800 was synthesized using a slight modification of the previous literature method (Yang et al., 2018; Zhang et al., 2018c). Briefly, $Ni(NO_3)_2{\cdot}6H_2O$ (2.823 g) and $Zn(NO_3)_2{\cdot}6H_2O$ (2.334 g) were dissolved into 20 mL of ultra-pure water, and NaOH was separately dissolved into 16 mL of ultra-pure water. After that, the two solutions were mixed to acquire a homogeneous solution. Immediately afterwards, HMeIM (2.580 g), MeOH (40 mL) and ammonia were poured into the resulting mixture under magnetic stirring for 1 h at room temperature. Subsequently, the precipitated product was collected and then washed with MeOH for several times. The obtained sample was dried at 60 °C under vacuum conditions for 8 h. After cooling to room temperature, it was ground into a powder. Finally, the sample was calcined in a horizontal quartz reactor at 800 °C for 8 h under a continuous flow of N_2 protection and the desired product was obtained.

2.2. Fabrication of modified electrode sensors

Before the modification, bare GCE was thoroughly polished on chamois leather with Al_2O_3 (0.3 and 0.05 μm) and rinsed several times with ultra-pure water until a mirror-like surface was acquired. Thereafter, the polished GCE was ultrasonicated successively with EtOH, nitric acid solution (v/v, 1:1) and ultrapure water for 5 min, respectively. Finally, the as-washed electrode was dried at room temperature for further use.

Herein, the poly caffeic acid (PCA)/GCE sensor was obtained by the electro-polymerization of caffeic acid (CAA) using Amperometric i-t Curve method at the potential of + 1.9 V for 600 s. After that, the as-prepared PCA/GCE sensor was placed in Zn/Ni-ZIF-8-800 suspension at the potential of − 0.6 V for 360 s to obtain the PCA@Zn/Ni-ZIF-8-800/GCE sensor using the same method. For comparison, the PCA/GCE sensor and Zn/Ni-ZIF-8-800/GCE sensor were constructed by using electro-polymerization of individual CAA or Zn/Ni-ZIF-8-800/GCE under the same conditions. The resulting electrode was rinsed with ultra-pure water and dried at room temperature for later electrochemical studies. The fabrication process of the PCA@Zn/Ni-ZIF-8-800/GCE sensor is shown in Scheme 1.

3. Results and discussion

3.1. Physical characterization

As shown in Fig. 1a, the XRD pattern of Zn/Ni-ZIF-8 shows main peaks at 7.2°, 10.4°, 12.6°, 14.7°, 16.6°, 18.0°, 22.0°, 24.4° and 29.5°, corresponding to the (011), (002), (112), (022), (013), (222), (114), (233), and (004) diffraction peaks, respectively (Li et al., 2014; Qu et al., 2017; Wang et al., 2016). It was also found that the main strong peaks of Zn/Ni-ZIF-8 were similar to those of pure ZIF-8, suggesting that the Zn/Ni-ZIF-8 was successfully prepared. In addition, the peaks of (022) and (222) in Zn/Ni-ZIF-8 displayed an obvious enhancement of relative intensities, while the peaks of (011) and (013) showed an weakness of relative intensities compare to ZIF-8, which can be attributed to the addition of Ni element. The XRD data were also in agreement with the reported literature (Wang et al., 2016). The XRD pattern of Zn/Ni-ZIF-8-800 displayed a broad peak around 25°, corresponding to carbon (002) diffraction, indicating the amorphous nature of Zn/Ni-ZIF-8-800.

The crystal sizes of ZIF-8, Zn/Ni-ZIF-8 and Zn/Ni-ZIF-8-800 were calculated to 21.0, 39.8 and 1.9 nm by use of Scherrer equation (D =

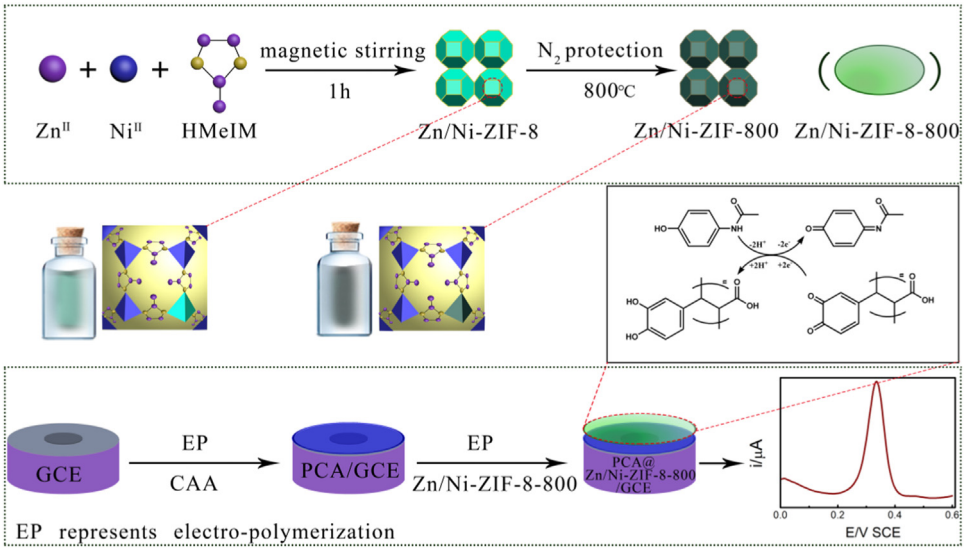

Scheme 1. The fabrication process of Zn/Ni-ZIF-8-800/GCE sensor, and the proposed mechanisms of AP at the prepared sensor.

$K\lambda/\beta\cos\theta$, Modi et al., 2018). Where D is the average crystallite size, K is the dimensionless shape factor (0.89), λ is the X-ray wavelength (0.15441 nm), β is the line broadening width at half maximum (FWHM) and θ is the Bragg angle. The crystal sizes of Zn/Ni-ZIF-8 were larger than ZIF-8, which is probably due to their faster crystal-growth rate in the presence of Ni element (Zhang et al., 2018c). Zn/Ni-ZIF-8–800 exhibited the smallest crystal sizes, which can be ascribed to the carbonization process of the organic compound in the Zn/Ni-ZIF-8 material.

Compared with the FT-IR spectrum of Zn/Ni-ZIF-8 (Supporting information Section S.2.1.1 and Fig. S.1), the absorption peaks of Zn/Ni-ZIF-8-800 (Fig. 1b) were located at 3376 cm^{-1}, 1670 cm^{-1}, 1136 cm^{-1} and 1060 cm^{-1}, respectively, demonstrating that the C-MOFs material retained the original framework structure of Zn/Ni-ZIF-8. Broad peaks of PCA at 3452 cm^{-1} and 1624.9 cm^{-1} could be attributed to the strong hydrogen bond interactions and C=C stretching vibration (Bai et al., 2018). The PCA@Zn/Ni-ZIF-8–800 material displayed the characteristic absorption peaks of both PCA and Zn/Ni-ZIF-8–800, confirming the formation of the desired hybrid modifier. Other characterizations of Zn/Ni-ZIF-8–800 were discussed in Supporting information Section S.2.1.2 and Figs. S.2–4.

The surface morphologies of the two different sensors were measured by SEM. It can be seen that PCA@Zn/Ni-ZIF-8-800/GCE sensor (Fig. 1e) displays a thicker, rougher and more irregular morphology than PCA/GCE (Fig. 1c), indicating that the hybrid film would be more beneficial for the electrochemical reaction of AP molecules. EDS (Fig. 1d and f) show that Ni and Zn existed in PCA@Zn/Ni-ZIF-8–800/GCE sensor but not in PCA/GCE sensor, further demonstrating that the

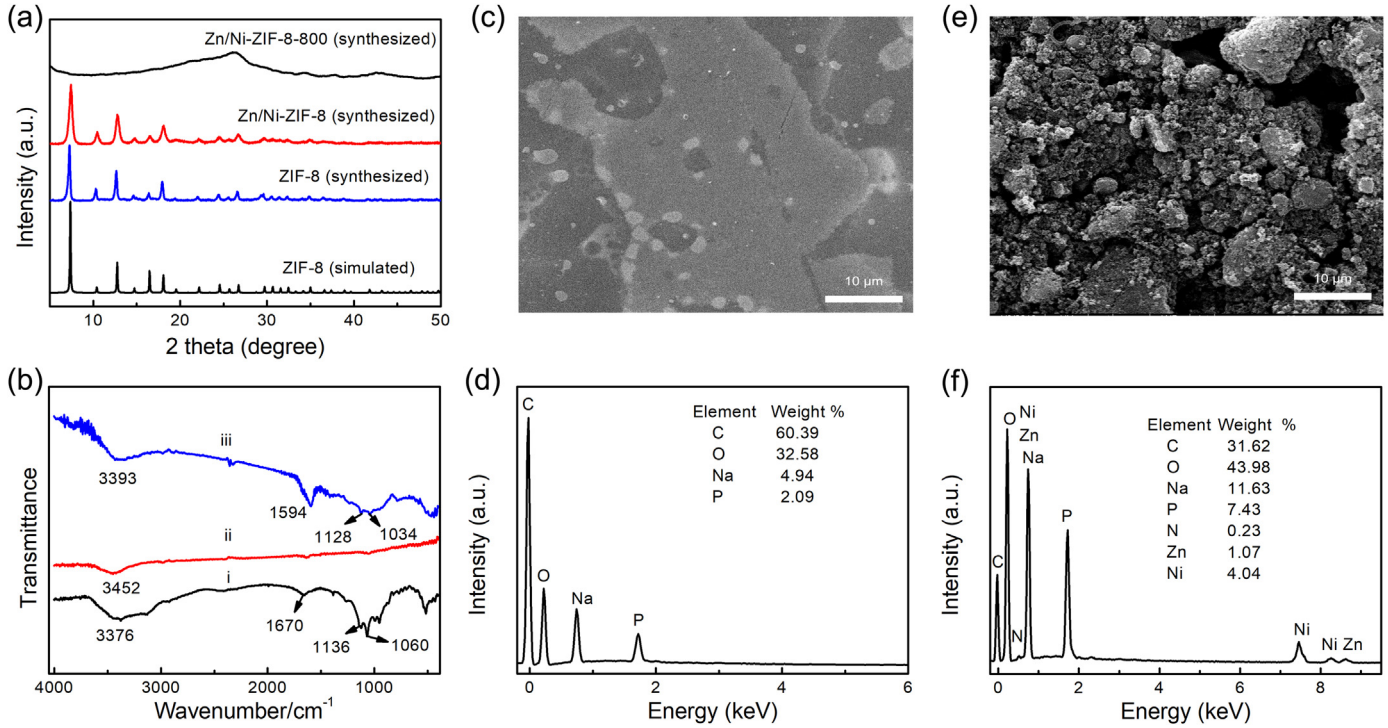

Fig. 1. (a) XRD patterns, and (b) FTIR spectra of Zn/Ni-ZIF-8–800, PCA and PCA@Zn/Ni-ZIF-8-800; (c) SEM and (d) EDS of PCA/GCE sensor; (e) SEM and (f) EDS of PCA@Zn/Ni-ZIF-8-800/GCE sensor.

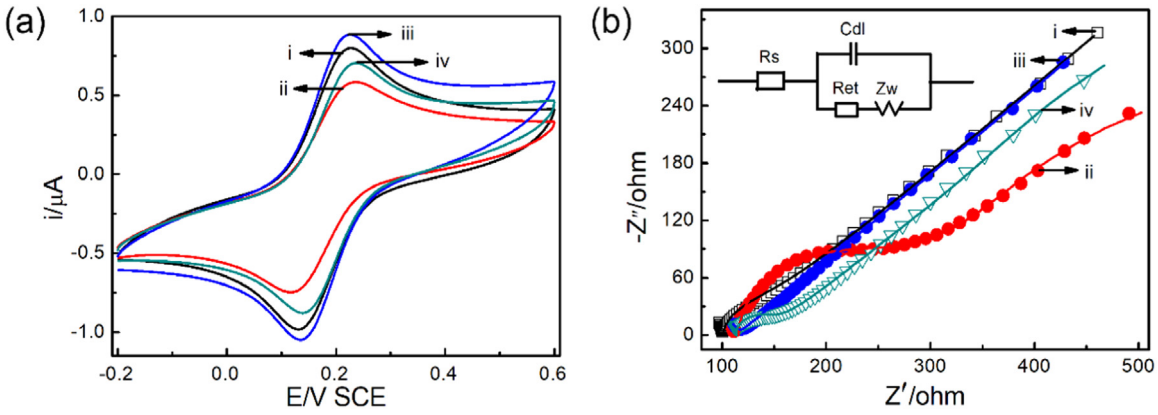

Fig. 2. (a) CVs and (b) EIS of bare GCE (i), PCA/GCE sensor (ii), Zn/Ni-ZIF-8-800/GCE sensor (iii), PCA@Zn/Ni-ZIF-8-800/GCE sensor (iv) in 0.1 M $Fe(CN)_6^{3-}$ containing 0.1 M KCl (inset: Randles equivalent circuit).

resulting materials were successfully coated onto the GCE.

3.2. Electrochemical characterization

CV is an effective technique to investigate the electron transfer ability of GCE and modified sensors. As presented in curve i of Fig. 2a, a pair of well-defined and reversible redox peaks were observed with the peak-to-peak separation (ΔE_p) of 93 mV (I_{pa} = 0.713 μA, I_{pc} = − 0.706 μA). After the electrode was modified with PCA (curve ii), the response current of $Fe(CN)_6^{3-}$ decreased (ΔE_p = 109 mV, I_{pa} = 0.512 μA, I_{pc} = − 0.504 μA), suggesting that the surface of PCA/GCE sensor was somewhat blocked because of the weak electron transfer ability of PCA. On the other hand, the current increased when Zn/Ni-ZIF-8-800 was polymerized on the GCE (curve iii, ΔE_p = 89 mV, I_{pa} = 0.754 μA, $I_{pc;}$ = − 0.794 μA), which can be attributed to the high conductivity of Zn/Ni-ZIF-8-800. As expected, the current of $Fe(CN)_6^{3-}$ at the PCA@Zn/Ni-ZIF-8-800/GCE sensor (curve iv, ΔE_p = 96 mV, I_{pa} = 0.612 μA, I_{pc} = − 0.659 μA) was higher than that at the PCA/GCE sensor, implying that the conductivity of PCA@Zn/Ni-ZIF-8–800 film was enhanced. The results indicate that Zn/Ni-ZIF-8-800 can provide enough electron transfer pathways in the interface between the proposed sensor and electrolyte solution.

Furthermore, EIS was employed to study the impedance change of the GCE and modified sensor surface, and the Nyquist plots are shown in Fig. 2b. In order to clearly understand the interface properties, the corresponding Randles equivalent circuit (inset of Fig. 2b) was utilized for fitting the impedance data by Z-view software. Rs, Ret, Cdl and Zw represent the uncompensated solution resistance, charge transfer resistance, double layer capacitance and Warburg impedance, respectively (Kim et al., 2010; Rezaei et al., 2014; Wei et al., 2018). The value of Ret reflects charge transfer resistance from the electron transfer process. The Ret values were found to be 32 Ω at GCE, 130 Ω at PCA/GCE sensor, 25 Ω at Zn/Ni-ZIF-8-800/GCE sensor, and 36 Ω at PCA@Zn/Ni-ZIF-8-800/GCE sensor, respectively. The EIS data were consistent with the CV results, further indicating the successful modification of the GCE with different materials. These results demonstrate that Zn/Ni-ZIF-8-800/GCE and PCA@Zn/Ni-ZIF-8-800/GCE films possess high conductivity and can be promising materials for electrochemical sensors. The corresponding CV and EIS data of Zn/Ni-ZIF-8 modified electrochemical sensors are also discussed in the Supporting information (Section S.2.1.3).

3.3. Electrochemical behavior of AP

The electrochemical behavior of AP at GCE and different modified sensors was investigated by CV method (Fig. 3a). For bare GCE (i), no obvious redox currents were observed in the potential range from 0.1 to 0.6 V. However, enhanced redox currents of AP at PCA/GCE sensor (curve ii, I_{pa} = 2.281 μA, I_{pc} = − 1.291 μA) and Zn/Ni-ZIF-8-800/GCE sensor (curve iii, I_{pa} = 4.032 μA, I_{pc} = − 2.093 μA) were observed, indicating that PCA and Zn/Ni-ZIF-8–800 obviously enhanced the current response of AP. The redox currents further increased when PCA@Zn/Ni-ZIF-8-800 was polymerized onto the GCE (I_{pa} = 6.079 μA, I_{pc} = − 3.039 μA), which can be ascribed to the good electrocatalytic effect of PCA towards AP, and the large surface area and good conductivity of Zn/Ni-ZIF-8-800. Therefore, the PCA@Zn/Ni-ZIF-8-800/GCE sensor is more efficient and applicable for the determination of AP. For comparison, the electrochemical performance of Zn/Ni-ZIF-8 modified electrode to fabricate corresponding sensor towards AP is presented in the Supporting information (Section S.2.1.4 and Fig. S.7). The results indicate that the calcination temperature of 800 °C for Zn/Ni-ZIF-8-800 material had a crucial effect on the electrochemical response of AP at the corresponding sensor.

The probable electrochemical reaction mechanism of AP at the PCA@Zn/Ni-ZIF-8–800/GCE sensor is presented as follows (Scheme 1): (i) The PCA exhibited good electrocatalytic activity, facilitating the reduction of AP to produce N-acetyl-p-quinone imine at the modified sensor; (ii) The Zn/Ni-ZIF-8-800 with large specific surface area provided a suitable microenvironment for the redox reaction of AP. Moreover, the material possessed superior conductivity due to the carbonization of the organic components of MOFs at the high temperature, which was beneficial for the electron transfer process. Furthermore, the electron-rich nature of Zn/Ni-ZIF-8-800 could facilitate electrostatic interaction between the surface of the modified sensor and AP; (iii) The enhanced electrochemical performance can be ascribed to the synergistic effect of PCA and Zn/Ni-ZIF-8-800, as well as the strong adsorption of AP molecules on the modified electrode sensor. The phenolic hydroxyl groups in the aromatic ring of PCA were oxidized to keto groups, by transferring two protons and electrons. Based on the reaction mechanism, the PCA@Zn/Ni-ZIF-8-800 sensor displayed excellent sensing performance for the determination of AP.

3.4. Optimization of the experimental conditions

3.4.1. Effect of the polymerization time

The effect of the polymerization time is discussed in the Supporting information (Section S.2.1.5, Fig. S.8).

3.4.2. Effect of pH value

The pH value of electrolyte solution played an important role in the response current of AP at the PCA@Zn/Ni-ZIF-8-800/GCE sensor. As displayed in Fig. S.9a, the redox peaks of AP were shifted towards negative side as the pH values increased from 5.0 to 8.0. The response current increased as the pH value increased up to 7.5, and then

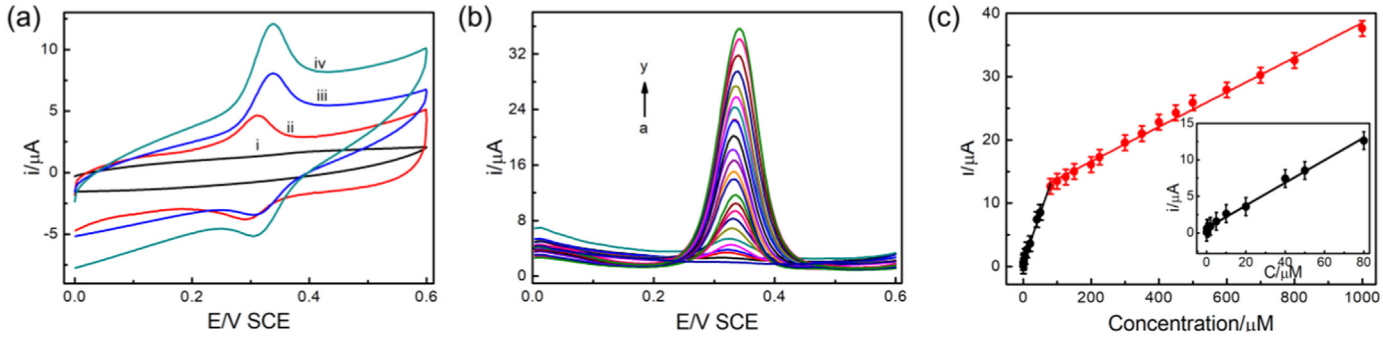

Fig. 3. (a) CVs of 0.1 mM AP in PBS (0.1 M, pH 7.5) at the bare GCE (i), PCA/GCE sensor (ii), Zn/Ni-ZIF-8-800/GCE sensor (iii), and PCA@Zn/Ni-ZIF-8-800/GCE sensor (iv), (b) DPVs obtained at the PCA@Zn/Ni-ZIF-8-800/GCE sensor in PBS (0.1 M, pH 7.5) containing different concentrations of AP (0.00–1000 μM), and (c) the corresponding linear relationship between redox peak currents and AP concentration. The inset is the enlarged calibration plot of AP at low concentrations (0.08 − 80 μM).

decreased when the pH exceeded 7.5 (Fig. S.9b), suggesting that a suitable acidity was helpful to the AP catalytic reaction.

As can be seen from Fig. S.9c, a pair of linear relationships between E_p and pH were obtained, and the regression equations were $E_{pa} = -0.0601\,pH + 0.781$ ($R^2 = 0.996$) and $E_{pc} = -0.0620\,pH + 0.761$ ($R^2 = 0.995$), respectively. The slope values of − 60.1 and − 62.0 mV/pH demonstrate that the number of protons and electrons participating in the redox reaction of AP were almost equal, and the electrochemical reaction of AP was a two-proton and two-electron process (Scheme 1). Similar behavior was observed in the determination of AP in the previous reports with different modified electrodes such as g-C_3N_4-E-PEDOT/GCE (Xu et al., 2018), MWCNT-βCD/GCE (Alam et al., 2018) and RGO-gold dendrite/GCE (Yu et al., 2018). Hence, pH 7.5 was chosen as the optimal pH value in the following experiments.

3.4.3. Effect of scan rate

The influence of scan rate on the response current of AP at the PCA@Zn/Ni-ZIF-8-800/GCE sensor was explored using CV method (Fig. S.10). As presented in Fig. S.10a, the redox peak current of AP increased as the scan rate increased ranging from 0.02 to 0.80 V s^{-1}. The corresponding linear relationship is displayed in Fig. S.10b, and the regression equations were I_{pa} (μA) = 94.254 v + 3.774 ($R^2 = 0.997$) and I_{pc} (μA) = − 65.929 v − 3.276 ($R^2 = 0.996$), respectively. The results indicate that the electrochemical reaction of AP at the modified sensor was a surface-controlled process involving van der Waals attraction. Similar electrochemical behavior has been reported in the previous literature (Lu and Tsai, 2011; Kutluay and Aslanoglu, 2013; Li et al., 2014; Fu et al., 2015). Moreover, the oxidation peak potentials shifted towards the positive side with increasing scan rate, while the corresponding reduction peak potentials shifted to more negative values. The linear relationships between peak potential and logarithm of the scan rates (log v) were expressed by the regression equations of $E_{pa} = 0.379 + 0.068 \log v$ (V s^{-1}, $R^2 = 0.993$) and $E_{pc} = 0.292 - 0.038 \log v$ (V s^{-1}, $R^2 = 0.987$), respectively (Fig. S.10c).

Furthermore, the electron-transfer kinetic parameters such as electron-transfer coefficient (α) and apparent charge-transfer rate constant (K_S) were calculated to be 0.636 and 4.68 s^{-1}. The detailed discussion is shown in Supporting information (Section S.2.1.7). According to the above results, 0.1 V s^{-1} was employed as the scan rate in the subsequent experiments.

3.5. Electrochemical response of the fabricated sensor for AP

The DPV responses of AP at the prepared sensor were investigated by varying the AP concentration. It can be seen that the oxidation peak current increased with the increase AP concentration in the range of 0.08–1000 μM (Fig. 3b). As shown in Fig. 3c, the response current was proportional to the concentration of AP, and the corresponding linear regression equations were I_1 (μA) = 0.659 + 1.155 C (C: μM, $R^2 = 0$ 0.994, 0.08–80 μM) with a sensitivity of 36.783 μA $μM^{-1}$ cm^{-2}, and I_2 (μA) = 11.084 + 0.0281 C (C: μM, $R^2 = 0.996$, 80–1000 μM) with a corresponding sensitivity of 0.892 μA $μM^{-1}$ cm^{-2}, respectively. The relative standard deviations (RSD) of 2.5% (n = 3) was obtained, indicating a high reproducibility of the proposed sensor. The phenomenon of two segments with different gradients was observed due to the different sensitivities of AP at the proposed sensor. The higher sensitivity at low AP concentration can be attributed to the adsorption-controlled process on the modified electrode sensor surface, which has been discussed in the previous section about effect of scan rate. In contrast, at higher AP concentration, excessive AP molecules gather on the polymer membrane, causing the collapse of the surface and the decrease in the number of active sites. Furthermore, the limit of detection (LOD) of AP was calculated to be 0.0291 μM as an average of the results from the above two regressions.

The reported results of other electrochemical sensors for detection of AP were compared with the modified sensor in this work, as shown in Table 1. The developed sensor in this work showed a wider linear range and lower detection limit for the determination of AP. The results demonstrate that the PCA@Zn/Ni-ZIF-8-800 film is a promising platform for the fabrication of electrochemical sensors, and the modified

Table 1
Comparison of different electrochemical sensors for the determination of AP.

Electrode snsors	Linear range (μM)	Detection limit (μM)	Recovery (%)	Reference
PANI-MWCNTs	1–100	0.25	94.60–104.00	Li, Jing (2007)
SWCNT-GNS/GCE	0.05–64.50	0.038	97.10–102.10	(Chen et al., 2012)
GR-CS/GCE	1.00–100.00	0.10	92.00–107.00	(Zheng et al., 2013)
MWCNT/GO/GCE	0.50–400.00	0.05	99.93–99.98	(Cheemalapati et al., 2013)
MWCNTs-GNS/GCE	0.80–110.00	0.10	99.90–100.80	(Arvand, Gholizadeh, 2013)
PSi/Pd-NS/CNTPE/GCE	0.40–353.50	0.10	98.00–105.00	(Ensafi et al., 2015)
LU/fMWCNT/MGCE	1.00–90.00	0.52	98.00–102.20	(Baghayeri, Namadchian, 2013)
CeBiOx NFs/SPE	2.30–130.00	0.20	96.00–102.00	(Cao et al., 2018)
PCA@Zn/Ni-ZIF-8-800/GCE	0.08–1000	0.029	98.52–106.73	This work

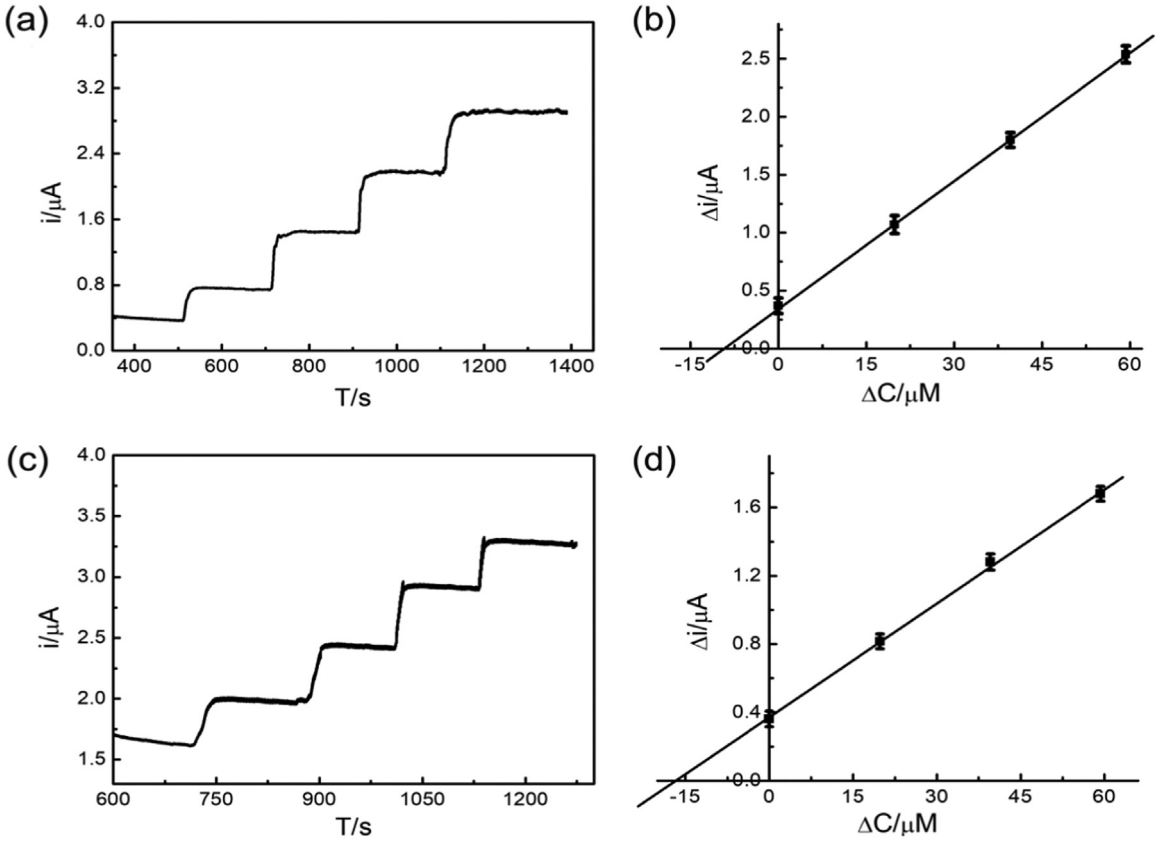

Fig. 4. (a) The amperometric responses of sequential additions of pharmaceutical reagent solution and three stitches of AP standard solution (each 20 μM per time; time interval = 200 s), and (b) the corresponding linear relationship of Δi versus ΔC of pharmaceutical dosage forms; (c) The amperometric responses of sequential additions of human urine real sample and three stitches of AP standard solution (each 20 μM per time; time interval = 150 s), and (d) the corresponding linear relationship of Δi versus ΔC of human urine real sample at the PCA@Zn/Ni-ZIF-8-800/GCE sensor in pH 7.5 PBS.

electrode sensor can detect AP in low concentrations with high sensitivity.

3.6. Reproducibility, stability and selectivity

The reproducibility, stability and selectivity are shown in the Supporting information (Section S.2.1.8, Fig. S.11).

3.7. Real sample analysis

To evaluate the feasibility of the proposed sensor for the practical determination of AP, the standard addition method was employed for measuring AP concentration in pharmaceutical dosage forms and human urine sample. The preparation procedures of the real samples have been described in Section S.1.4. Upward step trends were observed in the Amperometric i-t curve upon the successive additions of AP pharmaceutical reagent solution (or human urine real sample) and spiked AP solutions (Figs. 4a and 4c) in PBS (5 mL). The corresponding linear relationships of current change value (Δi) versus concentration change value (ΔC) were obtained as: ΔI_1 (μA) = 0.357 + 0.037 ΔC (Fig. 4b, R^2 = 0 0.999) and ΔI_2 (μA) = 0.370 + 0.023 ΔC (Fig. 4d, R^2 = 0.999), and the recoveries were calculated from the linear equations.

As shown in Supporting information (Section S.2.1.9 and Table S2), the recoveries for pharmaceutical dosage forms and human urine sample were in the ranges of 98.52–103.00% and 99.10–106.73%, respectively, suggesting that the proposed method offered good accuracy and reliability for the determination of AP in real samples.

4. Conclusions

In summary, a novel electrochemical sensor was successfully fabricated via electrochemical polymerization of CAA and Zn/Ni-ZIF-8-800 on the GCE surface for the determination of AP. Due to the excellent electrocatalytic activity of PCA, large surface area and high conductivity of Zn/Ni-ZIF-8-800 as well as the synergistic effect of PCA and Zn/Ni-ZIF-8-800, desirable electrochemical parameters were obtained for the PCA@Zn/Ni-ZIF-8-800 sensor such as wide linear range, low detection limit and high sensitivity towards AP. Furthermore, the prepared sensor exhibited better electrochemical parameters sensor than the previously reported sensors presented in the literature. The proposed method was applied for the determination of AP in pharmaceutical and urine samples with satisfactory recoveries. However, it is difficult and important to calculate the kinetic data between the MIP sensor and the AP molecules in this paper. Future work is in progress to develop more MOFs for electrochemical sensor applications and to calculate the kinetic and thermodynamic parameters of the corresponding sensors.

Acknowledgements

This work is financially supported by the National Natural Science Foundation of China (No. 51603062) and the High-level Talents Introduction Project of Henan Institute of Science and Technology (No. 210010617006).

Declaration of Interest Statement

None.

Appendix A. Supporting information

Supplementary data associated with this article can be found in the online version at doi:10.1016/j.bios.2019.01.069.

References

Adhikari, B., Govindhan, M., Chen, A., 2015. Electrochim. Acta 162, 198–204.
Alam, A., Qin, Y., Howlader, M.M.R., Hu, N., Deen, M.J., 2018. Sens. Actuators B-Chem. 254, 896–909.
Alothman, Z.A., Bukhari, N., Wabaidur, S.M., Haider, S., 2010. Sens. Actuators B-Chem. 146 (1), 314–320.
Arvand, M., Gholizadeh, T.M., 2013. Colloid Surf. B 103, 84–93.
Ates, M., 2013. Mat. Sci. Eng. C Mater. 33 (4), 1853–1859.
Baghayeri, M., Namadchian, M., 2013. Electrochim. Acta 108, 22–31.
Bai, R., Yu, Y., Wang, Q., Fan, X., Wang, P., Yuan, J., Shen, J., 2018. J. Clean. Prod. 191, 48–56.
Boopathi, M., Won, M.S., Shim, Y.B., 2004. Anal. Chim. Acta 512 (2), 191–197.
Cao, F., Dong, Q., Li, C., Chen, J., Ma, X., Huang, Y., Song, D., Ji, C., Lei, Y., 2018. Sens. Actuators B Chem. 256, 143–150.
Cernat, A., Tertis, M., Sandulescu, R., Bedioui, F., Cristea, A., Cristea, C., 2015. Anal. Chim. Acta 886, 16–28.
Chandra, P., Son, N.X., Noh, H.B., Goyal, R.N., Shim, Y.B., 2013. Biosens. Bioelectron. 39 (1), 139–144.
Cheemalapati, S., Palanisamy, S., Mani, V., Chen, S.M., 2013. Talanta 117, 297–304.
Chen, X., Zhang, G., Shi, L., Pan, S., Liu, W., Pan, H., 2016. Mat. Sci. Eng. C Mater. 65, 80–89.
Chen, X., Zhu, J., Xi, Q., Yang, W., 2012. Sens. Actuators B-Chem. 161 (1), 648–654.
Moatti Sirat, D., Velho, G., Reach, G., 1992. Biosens. Bioelectron. 7, 345–352.
Fu, L., Lai, G., Yu, A., 2015. RSC Adv. 5 (94), 76973–76978.
Glavanovic, S., Glavanovic, M., Tomisic, V., 2016. Spectrochim. Acta A 157, 258–264.
Habibi, B., Jahanbakhshi, M., Pournaghi Azar, M.H., 2011. Electrochim. Acta 56 (7), 2888–2894.
Vilchez, J.L., Blanc, R., Avidad, R., Navalón, A., 1995. J. Pharm. Biomed. 13, 1119–1125.
Juan-Juan, J., Marco-Lozar, J.P., Suárez-García, F., Cazorla-Amorós, D., Linares-Solano, A., 2010. Carbon 48 (10), 2906–2909.
Girish Kumar, K., Letha, R., 1997. J. Pharm. Biomed. 15, 1725–1728.
Karimi-Maleh, H., Ganjali, M.R., Norouzi, P., Bananezhad, A., 2017. Mat. Sci. Eng. C Mater. 73, 472–477.
Khan, N.A., Hasan, Z., Jhung, S.H., 2013. J. Hazard. Mater. 244–245, 444–456.
Kim, I.T., Shin, S., Shin, M.W., 2018. Carbon 135, 35–43.
Kim, Y.R., Bong, S., Kang, Y.J., Yang, Y., Mahajan, R.K., Kim, J.S., Kim, H., 2010. Biosens. Bioelectron. 25 (10), 2366–2369.
Kutluay, A., Aslanoglu, M., 2013. Sens. Actuators B Chem. 185, 398–404.
Lee, P.T., Compton, R.G., 2013. Electroanalysis 25 (7), 1613–1620.
Li, M., Jing, L., 2007. Electrochim. Acta 52 (9), 3250–3257.
Li, R., Ren, X., Feng, X., Li, X., Hu, C., Wang, B., 2014. Chem. Commun. 50 (52), 6894–6897.
Liu, B., Shioyama, H., Jiang, H., Zhang, X., Xu, Q., 2010. Carbon 48 (2), 456–463.
Lu, D., Zhang, Y., Wang, L., Lin, S., Wang, C., Chen, X., 2012. Talanta 88, 181–186.
Lu, T.L., Tsai, Y.C., 2011. Sens. Actuators B Chem. 153 (2), 439–444.
Mazloum-Ardakani, M., Beitollahi, H., Amini, M.K., Mirkhalaf, F., Abdollahi-Alibeik, M., 2010. Sens. Actuators B Chem. 151 (1), 243–249.
Modi, A., Verma, S.K., Bellare, J., 2018. Mat. Sci. Eng. C Mater. 91, 524–540.
Zidan, M., Zawawi, R.M., Erhayem, M., Salhin, A., 2014. Int. J. Electrochem. Sc. 9, 7605–7613.
Nebot, C., Gibb, S.W., Boyd, K.G., 2007. Anal. Chim. Acta 598 (1), 87–94.
Perez-Ruiz, T., Martinez-Lozano, C., Tomas, V., Galera, R., 2005. J. Pharm. Biomed. 38 (1), 87–93.
Qu, F., Zhang, B., Zhou, X., Jiang, H., Wang, C., Feng, X., Jiang, C., Yang, M., 2017. Sens. Actuators B Chem. 252, 649–656.
Rezaei, B., Khalili Boroujeni, M., Ensafi, A.A., 2014. Biosens. Bioelectron. 60, 77–83.
Ruengsitagoon, W., Liawruangrath, S., Townshend, A., 2006. Talanta 69 (4), 976–983.
Shi, X., Chen, Y., Lai, Y., Zhang, K., Li, J., Zhang, Z., 2017. Carbon 123, 250–258.
Sivakumar, M., Sakthivel, M., Chen, S.M., 2016. RSC Adv. 6 (106), 104227–104234.
Wang, H., Zhang, S., Li, S., Qu, J., 2018. Talanta 178, 188–194.
Wang, Y., Chen, B., Zhang, Y., Fu, L., Zhu, Y., Zhang, L., Wu, Y., 2016. Electrochim. Acta 213, 260–269.
Wang, S., Xie, F., Hu, R.F., 2007. Sens. Actuators B Chem. 123 (1), 495–500.
Wei, W., Dong, S., Huang, G., Xie, Q., Huang, T., 2018. Sens. Actuators B Chem. 260, 189–197.
Wu, S., Shen, X., Zhu, G., Zhou, H., Ji, Z., Ma, L., Xu, K., Yang, J., Yuan, A., 2017. Carbon 116, 68–76.
Xu, F., Ru, H., Sun, L., Zou, Y., Jiao, C., Wang, T., Zhang, J., Zheng, Q., Zhou, H., 2012. Biosens. Bioelectron. 38 (1), 27–30.
Xu, Y., Lei, W., Su, J., Hu, J., Yu, X., Zhou, T., Yang, Y., Mandler, D., Hao, Q., 2018. Electrochim. Acta 259, 994–1003.
Yu, S., Li, H., Li, G., Niu, L., Liu, W., Di, X., 2018. Talanta 184, 244–250.
Yang, H., Cui, W., Han, Y., Wang, B., 2018. Chin. Chem. Lett. 29 (6), 842–844.
Zhang, J., Xu, X., Chen, L., 2018a. Sens. Actuators B Chem. 261, 425–433.
Zhang, W., Xu, G., Liu, R., Chen, J., Li, X., Zhang, Y., Zhang, Y., 2016. Electrochim. Acta 211, 689–696.
Zhang, W., Zong, L., Geng, G., Li, Y., Zhang, Y., 2018b. Sens. Actuators B Chem. 257, 1099–1109.
Zhang, X., Zhang, T., Wang, Y., Li, J., Liu, C., Li, N., Liao, J., 2018c. J. Membr. Sci. 560, 38–46.
Zhao, R., Xia, W., Lin, C., Sun, J., Mahmood, A., Wang, Q., Qiu, B., Tabassum, H., Zou, R., 2017. Carbon 114, 284–290.